Mapping the groundwater vulnerability for pollution at the pan African scale

Article *in* Science of The Total Environment · February 2016
DOI: 10.1016/j.scitotenv.2015.11.135

3 authors:

Issoufou Ouedraogo
Université Catholique de Louvain
5 PUBLICATIONS **24** CITATIONS

Pierre Defourny
Université Catholique de Louvain
260 PUBLICATIONS **4,810** CITATIONS

Marnik Vanclooster
Université Catholique de Louvain
278 PUBLICATIONS **4,803** CITATIONS

Science of the Total Environment 544 (2016) 939–953

Contents lists available at ScienceDirect

Science of the Total Environment

journal homepage: www.elsevier.com/locate/scitotenv

Mapping the groundwater vulnerability for pollution at the pan African scale

Issoufou Ouedraogo *, Pierre Defourny, Marnik Vanclooster

Earth and Life Institute, Université catholique de Louvain, Croix du Sud 2, Box 2, B-1348 Louvain-la-Neuve, Belgium

HIGHLIGHTS

- Vulnerability and groundwater pollution risk were mapped at the African scale.
- Groundwater vulnerability and pollution are very heterogeneous at the African scale.
- Vulnerability maps are consistent with nitrate data inferred from a meta-analysis.

GRAPHICAL ABSTRACT

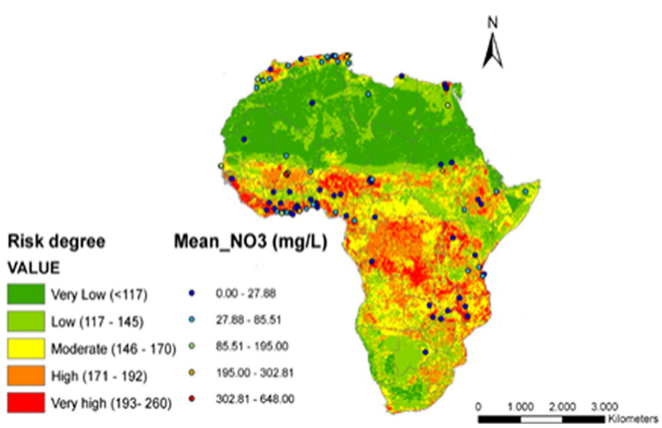

Spatial distribution of mean nitrate concentration in groundwater.

ARTICLE INFO

Article history:
Received 7 September 2015
Received in revised form 25 November 2015
Accepted 25 November 2015
Available online xxxx

Editor: D. Barcelo

Keywords:
Groundwater vulnerability
Nitrate contamination
Meta-analysis
Pollution risk

ABSTRACT

We estimated vulnerability and pollution risk of groundwater at the pan-African scale. We therefore compiled the most recent continental scale information on soil, land use, geology, hydrogeology and climate in a Geographical Information System (GIS) at a resolution of 15 km × 15 km and at the scale of 1:60,000,000. The groundwater vulnerability map was constructed by means of the DRASTIC method. The map reveals that groundwater is highly vulnerable in Central and West Africa, where the watertable is very low. In addition, very low vulnerability is found in the large sedimentary basins of the African deserts where groundwater is situated in very deep aquifers. The groundwater pollution risk map is obtained by overlaying the DRASTIC vulnerability map with land use. The northern, central and western part of the African continent is dominated by high pollution risk classes and this is very strongly related to shallow groundwater systems and the development of agricultural activities. Subsequently, we performed a sensitivity analysis to evaluate the relative importance of each parameter on groundwater vulnerability and pollution risk. The sensitivity analysis indicated that the removal of the impact of vadose zone, the depth of the groundwater, the hydraulic conductivity and the net recharge causes a large variation in the mapped vulnerability and pollution risk. The mapping model was validated using nitrate concentration data of groundwater as a proxy of pollution risk. Pan-African concentration data were inferred from a meta-analysis of literature data. Results shows a good match between nitrate concentration and the groundwater pollution risk classes. The pan African assessment of groundwater vulnerability and pollution risk is expected to be of particular value for water policy and for designing groundwater resources management programs. We expect,

* Corresponding author.
E-mail address: ouediss6@yahoo.fr (I. Ouedraogo).

http://dx.doi.org/10.1016/j.scitotenv.2015.11.135

however, that this assessment can be strongly improved when better pan African monitoring data related to groundwater pollution will be integrated in the assessment methodology.

1. Introduction

Groundwater is an important water resource for meeting the various water demands in Africa. It is vital for supporting the socio-economic development of the continent, as well as for maintaining a wide diversity of ecosystem functions and services. However, the booming population in Africa, together with climate change, increase the pressure on the African groundwater resources considerably, both in quantity as in quality. For defining sustainable water resources management plans at the continental scale, assessments of groundwater resources and associated pressures are strongly needed (Hasiniaina et al., 2010).

Several studies have already been undertaken to improve the knowledge of African groundwater systems. At the local scale, Xu and Usher (2006) recently compiled information from the UNEP/UNESCO project "Assessment of pollution Status and Vulnerability of Water Supply Aquifers of African Cities". They confirm that groundwater in African cities is subjected to different pollution pressure exerted by several sources such as leaking sewage systems, solid waste dumpsites, household waste pits, surface water infiltration spots, peri-urban agriculture sites, petrol service stations (underground storage tanks) and wellfields. According Xu and Usher (2006), the major issues of water quality in Africa can be listed in order of importance as follows: (1) nitrate pollution, (2) pathogenic agents, (3) organic pollution, (4) salinization, and (5) acid mine drainage. At the continent scale, studies include the development of the African groundwater map (WHYMAP, 2008; Seguin, 2008), the assessment of groundwater potential (Wright, 1992; Chilton and Foster, 1995), the assessment of basin yield, storage capacity, flow types and saturated thickness (Bonsor and MacDonald, 2011), the drought vulnerability in the SADC region (Villholth et al., 2013), the groundwater availability (UNEP, 2010; Pavelic et al., 2012) and the irrigation potential from renewable groundwater (Altchenko and Villholth, 2014). More recently, studies were also undertaken at the global scale. de Graaf et al. (2014), for instance, presented the first high-resolution global scale groundwater model. Notwithstanding this recent progress, no study has been made for assessing the pan African scale groundwater vulnerability for pollution. Assessing groundwater quality at the large scale is particularly important for monitoring progress in sustainable development, such as the implementation of the UN SDG for water.

In this context, assessing the groundwater vulnerability for pollution is important for designing efficient regional scale groundwater management and protection strategies. When discussing groundwater vulnerability, a difference can be made between specific vulnerability and intrinsic vulnerability (NRC, 1993). Intrinsic vulnerability of an aquifer can be defined as the capacity with which a contaminant introduced at the ground surface can reach and diffuse in groundwater (Vrba and Zaporozec, 1994). Specific vulnerability is used to define the vulnerability of groundwater to a particular contaminant or a group of contaminants. For specific vulnerability, specific physico-chemical properties from contaminants are considered (Gogu and Dassargues, 2000). Groundwater pollution risk can be defined as the process of estimating the possibility that a particular event may occur under a given set of circumstances (Voudouris, 2009) and the assessment is achieved by overlaying hazard and vulnerability (Gogu and Dassargues, 2000; Uricchio et al., 2004). Several approaches exist for assessing groundwater vulnerability. They can be grouped into methods based on the use of (1) process-based simulation models, (2) statistical models and (3) overlay and index methods (Al-Hanbali and Kondoh, 2008; Gogu and Dassargues, 2000; Farjad et al., 2012; Mimi et al., 2011). Alternatively, they can be classified according the degree of integration of monitoring data in the vulnerability assessment (Vanclooster et al., 2014). Hence, distinction can be made between vulnerability assessment methods based on generic data, based on groundwater monitoring data, or hybrid methods based both on monitoring and generic data.

Within the class of generic data based methods, the most established method worldwide is the DRASTIC method (Aller et al., 1985, 1987). The method has been widely used for regional vulnerability assessments in many countries such as the USA (Fritch et al., 2000; Shukla et al., 2000), China (Mao et al., 2006), Canada (Liggett and Gilchrist, 2010), India (Senthilkumar et al., 2014), Turkey (Ersoy and Gültekin, 2013), Tunisia (Saidi et al., 2010, 2011), South Africa (Musekiwa and Majola, 2013) and Ivory Coast (Jourda et al., 2007), among many others. The DRASTIC method, as like similar index models, has many advantages: (1) the method has a low cost of application and can be applied at the regional scale, because it is based on often easily available generic data (Aller et al., 1987); and (2) the use of a high number of input data layers is believed to limit the support of errors or uncertainties of the individual data layer in the final output (Evans and Myers, 1990, Rosen, 1994). Despite its popularity, the DRASTIC method has some disadvantages (Neshat et al., 2014). First, many variables are factored into the vulnerability index. All these factors are not necessarily sensitive for groundwater vulnerability for a particular setting (Vbra and Zaporozec, 1994). Hence, in many cases vulnerability can be explained with a subset of DRASTIC factors. Second, studies based on the DRASTIC method tend to overestimate the vulnerability of porous media aquifers compared to aquifers of fractured media (Rosen, 1994). Third, only few studies have been performed to validate the DRASTIC vulnerability method at the regional scale. Despite these disadvantages, the DRASTIC method can easily be deployed to make continental scale assessment of groundwater vulnerability.

The major objective of this study is to assess the groundwater vulnerability and pollution risk at the pan African scale, using the DRASTIC indicator methodology. A specific objective are to identify the quality and sensitivity of the different data layers in the regional scale vulnerability assessment and to assess the validity of the vulnerability assessment using nitrate contamination as a proxy of the vulnerability. To implement the DRASTIC indicator methodology at the pan African scale, a high quality environmental data base for the continent was established.

2. Study area

Africa, after Australia, is the world's second-driest continent. With about 15% of the global population, it has only 9% of global renewable water resources that are either abundant or scarce, depending on the season or the place. Furthermore, water is a crucial element in ensuring livelihoods since more than 40% of Africa's population lives in arid, semi-arid and dry sub-humid areas and about 60% live in rural areas and depend mainly on rain-fed agriculture for their livelihoods (UNEP, 2010). Madagascar was masked out in the final map due to the lack complete data for this region. According Ateawung (2010), the relief of Africa is characterized by two broad elevated regions of eastern and southern Africa, having an average height of 1015 m asl. The African continent encompasses various climate regions and a large diversity in geology. MacDonald et al. (2011) distinguishes five important hydrogeological environments: pre-cambrian crystalline basement rocks (34% of total area), consolidated sedimentary rocks (37% of total area), volcanic rocks (4% of total area), unconsolidated sediments (approximately 25% of total area) and unconsolidated sediments in river valleys (probably less than 1% of total area). The latter two hydrogeological environments definitely encompass the most

Table 1
Weight settings for DRASTIC parameters (Aller et al., 1987).

Symbol	Parameter	Weight
D_w	Depth to water	5
R_w	Net recharge	4
A_w	Aquifer media	3
S_w	Soil type	2
T_w	Topography	1
I_w	Impact of vadose zone	5
C_w	Hydraulic conductivity	3

productive aquifers. Eighty important aquifers in Africa are transboundary aquifers (Altchenko and Villholth, 2013). The total groundwater storage is estimated in Africa at 0.66 million km^3 with a range in uncertainty of between 0.36 and 1.75 million km^3 (MacDonald et al., 2012).

3. Materials and methods

3.1. The DRASTIC model

In the present study, the DRASTIC method is used for evaluating groundwater vulnerability for pollution. The acronym DRASTIC corresponds to the initials of the seven variables that drives vulnerability as defined according to Aller et al. (1987) and shown in Table 1.

The DRASTIC vulnerability index was calculated by the addition of the different products (rating × weight of the corresponding parameter), using the following the equation:

$$D_i = D_w D_{r,i} + R_w R_{r,i} + A_w A_{r,i} + S_w S_{r,i} + T_w T_{r,i} + I_w I_{r,i} + C_w C_{r,i} \quad (1)$$

where Di, is the DRASTIC index; D, R, A, S, T, I, and C are the seven parameters, as defined in Table 1; and the subscripts r, i and w are the corresponding rating for grid cell i and weights.

The weights indicate the relative importance of each DRASTIC parameter with respect to the other parameters. These weights are constant (Ehteshami et al., 1991). Also, for each DRASTIC parameter, the designated rating varies from 1 to 10. The rating ranges were determined depending on the properties at the pan-African scale. A good knowledge of geology and hydrogeology of the research area is a prerequisite to determine the rating ranges of the parameters (Sener et al., 2009). In general, the ratings assigned in this study were similar to the typical ratings suggested in the original DRASTIC study (Aller et al., 1987). However, they have been adjusted to consider the full variability of DRASTIC parameters as retrieved in the present study (Tables 4 and 5), similarly as in the example presented by Sener et al. (2009).

Finally, for purposes of interpretation, we subdivided the possible values of the DRASTIC index calculated into five classes of vulnerability, according to the range of indices defined by Jourda et al. (2007):

— Di > 176 is considered to have a very high vulnerability;
— 146 < Di < 175 is considered to have a high vulnerability;
— 115 < Di < 145 is considered to have a moderate vulnerability;
— 84 < Di < 114 is considered to have a low vulnerability; and
— Di < 84 is considered to have a very low vulnerability.

3.2. Data acquisition and data base compilation

We constructed a GIS database for the hydrogeology, the geology, the soil, the groundwater recharge and topography of Africa. Table 2 shows the metadata of the constructed GIS database. We processed all data with ArcGIS 10.2™, QGIS™ $^{2.2}$ and Matlab™.

Data came in various spatial resolutions. We resampled data layers to be suitable with the proposed resolution of the GIS model. We proposed a 15 km × 15 km resolution for this study. We consider that this resolution is a reasonable compromise between different resolutions of the different datasets, computing constraints and regional extent. We obtained the vulnerability and risk maps, after classifying and assigning relative ratings and weights, then overlaying the individual maps in a GIS.

3.3. Development of the DRASTIC parameters

Fig. 1 gives an overview of the methodology used to develop the intrinsic groundwater vulnerability map. Each parameter processed in the GIS is described below.

3.3.1. Depth of groundwater (D)

The 'Depth to water table' (D), is the vertical distance from the land surface to the top of the saturated zone in the aquifer. It represents the distance that a potential contaminant must travel before reaching the aquifer. Consequently, the D will have an impact on the degree of interaction between the percolating contaminant and the sub-surface materials (air, minerals, water) and, therefore, on the degree and extent of the physical and chemical attenuation and the degradation process (Rahman, 2008). In general, the vulnerability for pollution decreases with D. The D was calculated from the data as presented by Bonsor and MacDonald (2011). The original value of this parameter was not continuous and was obtained in a categorical data format.

3.3.2. Net Recharge (R)

The 'Net Recharge', R, represents the amount of water per unit area of land penetrating the ground surface and reaching the water table. It is thus influenced by the amount of surface cover, the slope of the

Table 2
Data used for the creation of the seven parameter data layers of the pan African DRASTIC model.

Raw data	Sources	Format	Resolution/scale	Date	Output layer
Depth to groundwater map	British Geological Survey (http://www.bgs.ac.uk/)	xyzASCII file	5 km	2012	Depth of water (D)
Recharge data	P.Döll and F. Portman (University of Frankfurt)	Shapefile	0.5°×0.5°	2008	Recharge (R)
The new global lithological map database (GLiM)	Nils Moosdorf (Hamburg University)	File Geodatabase feature	1:3,750,000	2012	Aquifer media (A)
Soil data	ISRIC, World Soil Information	Raster	1 km × 1 km	2014	Soil type (S)
SRTM90	UCL/ELIe-Geomatics (Belgium) and CGIAR/CSI	Raster	90 m × 90 m	2000	Topography (T) or slope (%)
The new global lithological map(GLiM)	Nils Moosdorf (Hamburg University)	File Geodatabase feature	1:3,750,000	2012	Impact of Vadose zone (I)
Global HYdrogeologyMaPS (GLYMPS) of permeability and porosity	T;P;Gleeson (McGill University)	File Geodatabase feature	Average size of polygon ~ 100 km^2	2014	Hydraulic Conductivity (C)
Land cover/land use map	UCL/ELIe-Geomatics (Belgium)	Raster geotiff	300mx300m	2014	Land Use (LU)

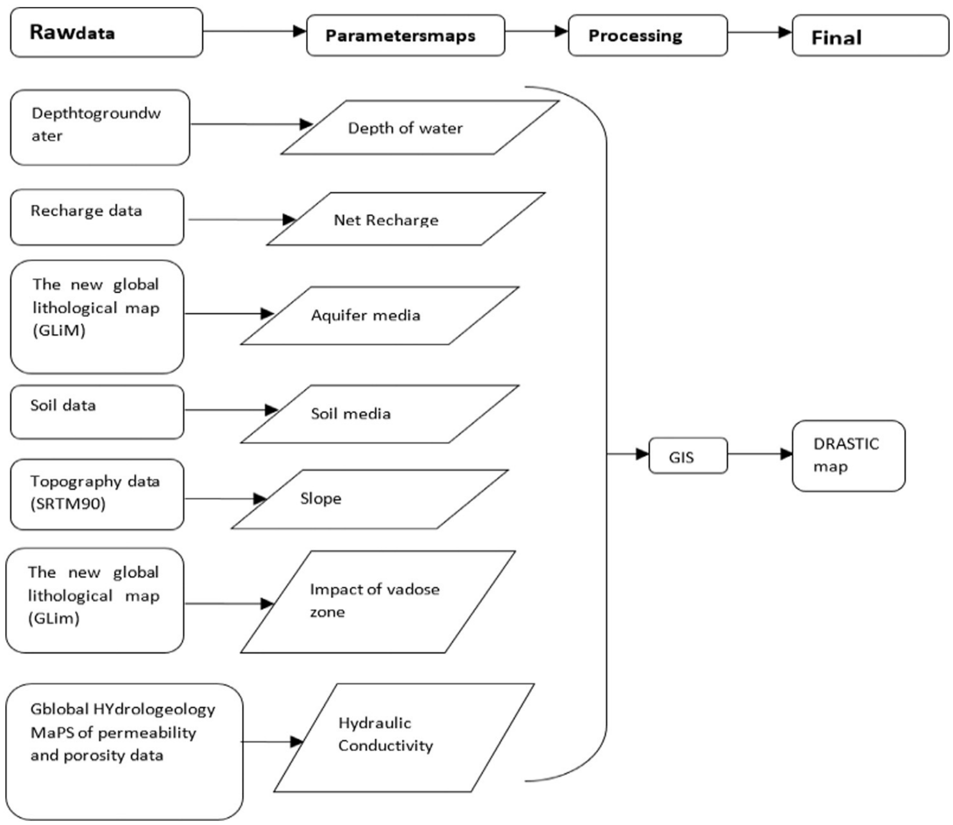

Fig. 1. Flow chart of the methodology used to develop the groundwater vulnerability map using the DRASTIC model in GIS.

land surface, the permeability of the soil and the amount of water that recharge the aquifer. The dispersion and dilution of contaminants depend greatly on the volume of water available in the vadose zone as well as in the saturated zone and thus on the net recharge. High recharge areas are more vulnerable than low recharge areas. Net recharge was derived from the global-scale modeling of groundwater recharge as presented by Döll and Fiedler (2008).

3.3.3. Aquifer media (A)

The 'Aquifer media', *A*, refers to type of consolidated or unconsolidated material which hosts the aquifer (Ersoy and Gültekin, 2013). *A* was inferred from three main data sources: (1) the high resolution global lithological database (GliM) of Hartmann and Moosdorf (2012); (2) the global permeability estimates of Gleeson et al. (2011); and (3) the African hydrogeology and rural water supply map of

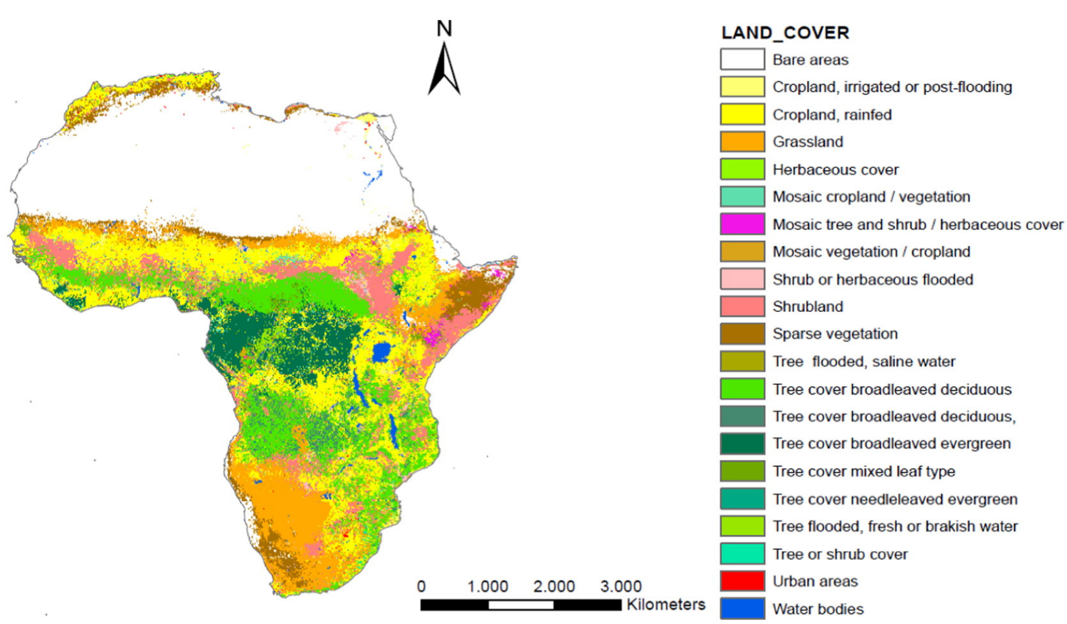

Fig. 2. Land cover/land use map for Africa.

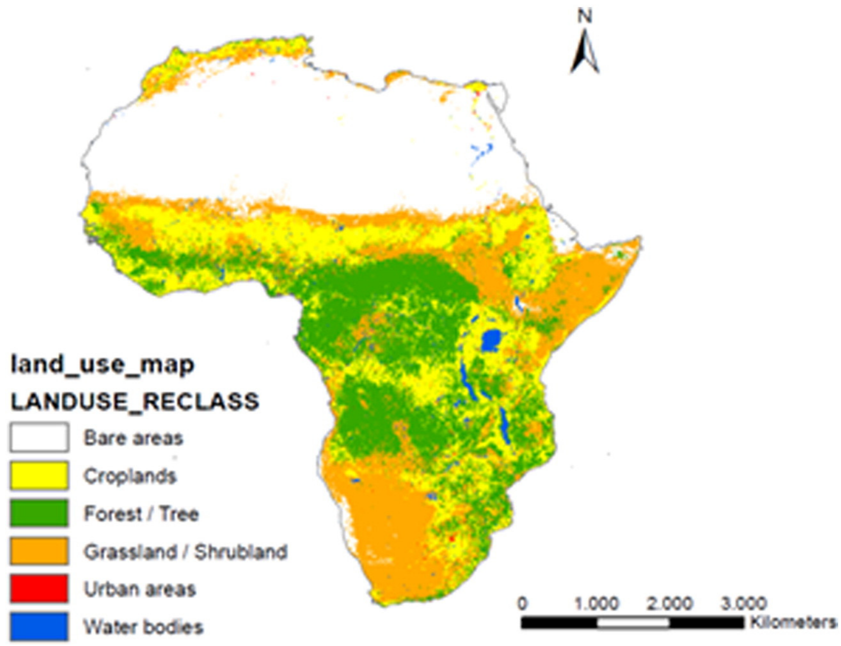

Fig. 3. Categories of land cover/land use map.

MacDonald et al. (2008). The analysis of the global permeability has permitted to identify parent material for each hydrolithologic unit. The GLiM databases encompass 16 lithological classes, is similar to the number of classes as used in the study of Dürr et al. (2005). In this work, we assumed that the lithological map represents the geology. Aquifer media were determined of each of the five hydrolithologies, defined as broad lithologic categories with similar hydrogeological characteristics (Gleeson et al., 2011). These categories are unconsolidated sediments, siliciclastic sediments, carbonate rocks, crystalline rocks and volcanic rocks (Gleeson et al., 2014). Aquifer media and Impact of vadose zone were inferred from GLiM and global permeability data. The vulnerability of the aquifer will increase if the grain size and the fractures or openings within the aquifer will increase (Alwathaf, 2011).

3.3.4. Impact of the vadose zone (I)

The role of the unsatured zone above the water table is integrated in the I parameter. It is an important parameter in the estimation of vulnerability, because it influences the residence time of pollutants in the unsaturated zone, and hence the attenuation probability. Similar to the A parameter, the method used to identify the vadose zone material depend on GLiM data and the African hydrogeological map, based on each parent material type that is the same as for aquifer media. The weights and ratings for I are shown in Table 4 and Fig. 7, and correspond to the map layer created for the vadose zone.

3.3.5. Topography (T)

The'Topography', T, determines the runoff and infiltration capacity of the surface water into the soil, and hence the capacity to introduce pollutants into the soil. If the slope is important, more runoff will be generated and hence groundwater contamination risk will be low. However, flat areas tend to retain water for a long time, therefore increasing the potential for migration of contaminants. The T was inferred from the 90 meter Shuttle Radar Topography Mission (SRTM90) database. The slope values were generated with the SRTM 90 by using the Spatial Analyst software of ArcGIS10.2TM. The slope layers were resampled and reclassified with the ratings into six classes.

3.3.6. Soil media (S)

Soil is the first media the contaminant passes through when it percolates into the ground. According to Lee (2003), soil has a significant impact on the amount of recharge that can infiltrate into the ground, and hence on the ability of a contaminant to move vertically into the vadose zone. For this study, the soil map of Africa was inferred from the data processed by Hengl et al. (2014).

3.3.7. Hydraulic conductivity (C)

The 'Hydraulic conductivity', C, is a measure of the ability of the aquifer to transmit water when submitted to a hydraulic gradient. It determines the migration velocity of pollutants, and hence the residence time and attenuation potential. High conductivity values will be associated to high contamination risks (Rahman, 2008). We inferred the hydraulic conductivity map from the global hydrogeological map of permeability and porosity, as produced by Gleeson et al. (2014). This global permeability map is given in log permeability (log (k)). From our case, the hydraulic conductivity is more useful. We converted k permeability into K hydraulic conductivity as follows:

$$K = k * rho * g/mu \qquad (2)$$

where K (m/s) is hydraulic conductivity which depends on fluid viscosity and density, rho (kg/m^3) is the density of the fluid, normally water = 999.97 kg/m^3, g (m/s^2) is the acceleration due to gravity = 9.8 m/s^2;

Table 3
Rating of land use in this study.

Land cover/Land use	Rating
Urban[a]	8
Croplands[b]	10
Grassland/shrubland[b]	4
Tree/forest[c]	1
Water bodies[a]	3
Bare areas[d]	1

[a] After: Bataineh et al.
[b] After: Dickerson (2007).
[c] After: Secunda et al. (1998).
[d] After: from Shirazi et al. (2012).

Table 4
Rate and weight of the seven DRASTIC parameters (Aller et al., 1987).

Depth of Groundwater (m)		Net Recharge (mm)		Topography (%)		Hydraulic Conductivity (m/day)		Soil media	
Interval	Ratings	Interval	Ratings	Interval	Ratings	Interval	Ratings	Soil classes	Ratings
0–7	10	0–45	1	0–2	10	<=0.010426	1	Clay	1
7–25	8	45–123	3	2–4	9	0.010426–0.038255	2	Clay loam	3
25–50	5	123–224	6	4–8	8	0.038255–0.12701	4	Loam	5
50–100	3	224–355	8	8–12	5	0.12701–0.34525	6	Loamy sand	7
100–250	2	>355	9	12–18	3	0.34525–0.569221	8	Sandy clay	2
>250	1			>18	1	0.569221–2.819372	10	Sandy clay loam	4
								Sandy loam	6
								Silty clay loam	3
								Sand	9
Weight:5		Weight: 4		Weight: 1		Weight: 3		Weight: 2	

and mu (kg/m.s or Pa.s) is the viscosity of the fluid. Hence, following Gleeson et al. (2014), we use the following conversion:

$$K = k * 1e + 7 \quad (3)$$

3.4. Sensitivity analysis

One of the major advantages of the DRASTIC model is the fact that a high number of input data layers is used (Evans and Myers, 1990). Indeed, increasing the number of data layers limits the impact of errors or uncertainties of the individual parameters on the final output (Rosen, 1994). Some scientists agreed that groundwater vulnerability assessment can be studied without considering all the factors of the DRASTIC model (Merchant, 1994); yet this opinion is not shared by others (e.g. Napolitano and Fabbri 1996). We therefore performed a sensitivity analysis that provides information on the influence of rating and weights assigned to each of the factors considered in the model (Gogu and Dassargues 2000).

Two sensitivity analyses tests were performed: the map removal sensitivity analysis introduced by Lodwick et al. (1990), and the single parameter sensitivity analysis introduced by Napolitano and Fabbri (1996).

The map removal sensitivity identifies the sensitivity of the vulnerability map towards removing one or more maps from the analysis and is computed by the following equation:

$$Si = (|Di/N - D'i/n|/Di) \times 100 \quad (4)$$

where Si is the sensitivity index, Di is the unperturbated vulnerability index, D′i is the perturbated vulnerability index, i is the grid cell index, and N and n are the number of data layers used to calculate Di and D′i. We considered the vulnerability index obtained using all the seven parameters as an unperturbated vulnerability index and the vulnerability computed using fewer parameters layers as the perturbated vulnerability.

The single-parameter sensitivity measure was developed to evaluate the impact of each of the DRASTIC parameters on the vulnerability index. It allows comparing the “effective” weight with their “theorical” weight (Babiker et al., 2005). The “effective” weight of each parameter in each subarea is computed using the following equation:

$$Wi = (P_{r,i} \times P_w/Di) \times 100 \quad (5)$$

where Wi refers to the “effective” weight of each parameter, $P_{r,i}$ and P_w are the rating value and the weight of each parameter respectively, and Di is the overall vulnerability index.

3.5. Development of groundwater risk map

The groundwater pollution risk corresponds to the potential of a groundwater body for undergoing groundwater contamination (Farjad et al., 2012). The risk of pollution is determined both by the intrinsic vulnerability of the aquifer, which is relatively static, and the existence of potentially polluting activities at the soil surface. These latter activities

Table 5
Rate and weights (A = 3 and I = 5) of aquifer media and impact of the vadose zone (Aller et al., 1987).

Lithology classes[a]	Hydrolithology classes[b]	Bedrock material	A and I ratings
Unconsolidated sediments	Unconsolidated		8
	c.g. unconsolidated	Alluvial deposits, dune sands	
	f.g. unconsolidated	Loess (Aeolian sediment), organic sediment	
Siliciclastic sediments	Siliciclastic sedimentary	Limestone, sandstone,	6
	c.g. siliciclastic sedimentary	Dolomite, siltstone, salt	
	f.g. sedimentary	Conglomerate, shale	
Mixed sedimentary rocks	Carbonate	Karst limestone	10
Carbonate sedimentary rocks			
Evaporites			
Acid volcanicrocks	Volcanic	Permeable basalt	9
Intermediate volcanic rocks			
Basic volcanicrocks			
Acid plutonic rocks	Crystalline	Igneous/metamorphic rocks	A(3) and I(4)
Intermediate plutonic rock			
Basic plutonic rocks			
Metamorphic rocks			
Water bodies	«Others rock»	–	8

[a] Hartmann and Moosdorf (2012).
[b] Based on Gleeson et al. (2011).

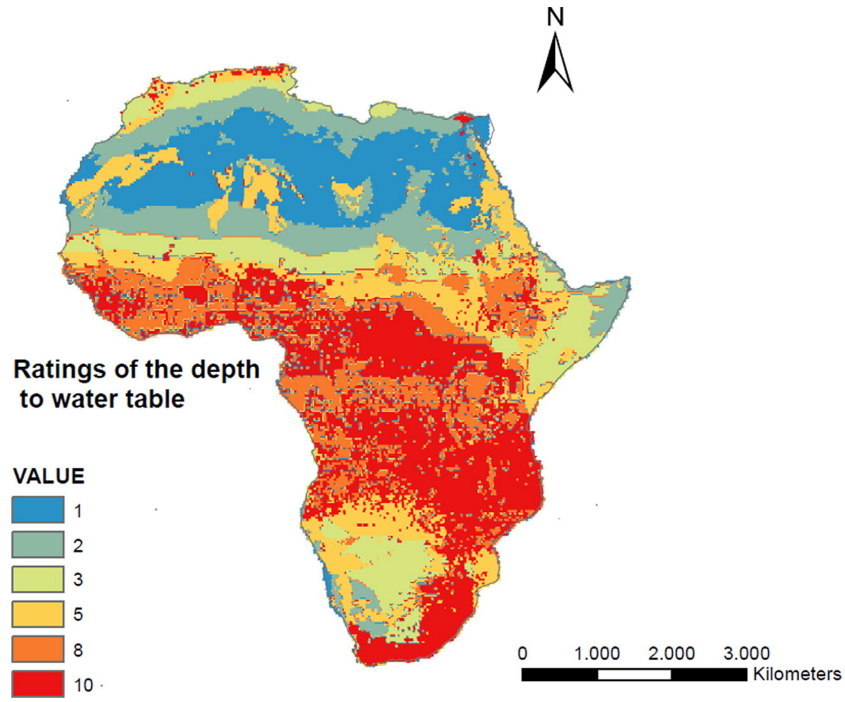

Fig. 4. DRASTIC rating for the depth to groundwater (D) for Africa.

are time dynamic and can be controlled (Saidi et al., 2010). Land use information is often used as a proxy for pollution pressure at the soil surface. In this study, the high resolution land cover/land use map was obtained from the GlobCoverdatat set (Mayaux et al., 2003). We used the land use categories as defined by Mayaux et al. (2003). Land use is thus grouped into five classes namely (1) forests, (2) woodlands, shrub lands and grasslands, (3) agriculture, (4) bare soil and (5) other land-cover classes (water bodies and cities). We generated the groundwater pollution risk map by combining the intrinsic groundwater vulnerability map with the land use map, using the additive model of Secunda et al. (1998).

Hence, the land use (L) is incorporated here into the risk model as an eighth parameter. Using the following DRASTIC equation, modified from Secunda et al.(1998):

$$MD_i = D_i + L_{r,i} \times L_w \tag{6}$$

where MD_i is the modified DRASTIC index for risk assessment, D_i is the DRASTIC index and $L_{r,i} \times L_w$ is the multiplication of rating for grid cell i and weight for land use.

In order to evaluate the groundwater pollution risk map at the pan African scale, the land use/land cover map was combined with the

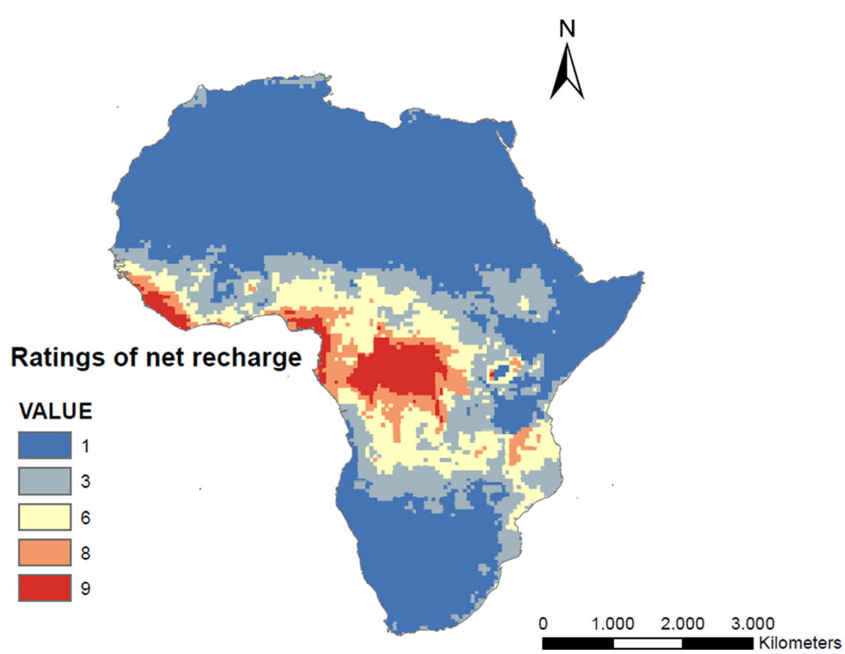

Fig. 5. DRASTIC ratings for the net recharge (R) for Africa.

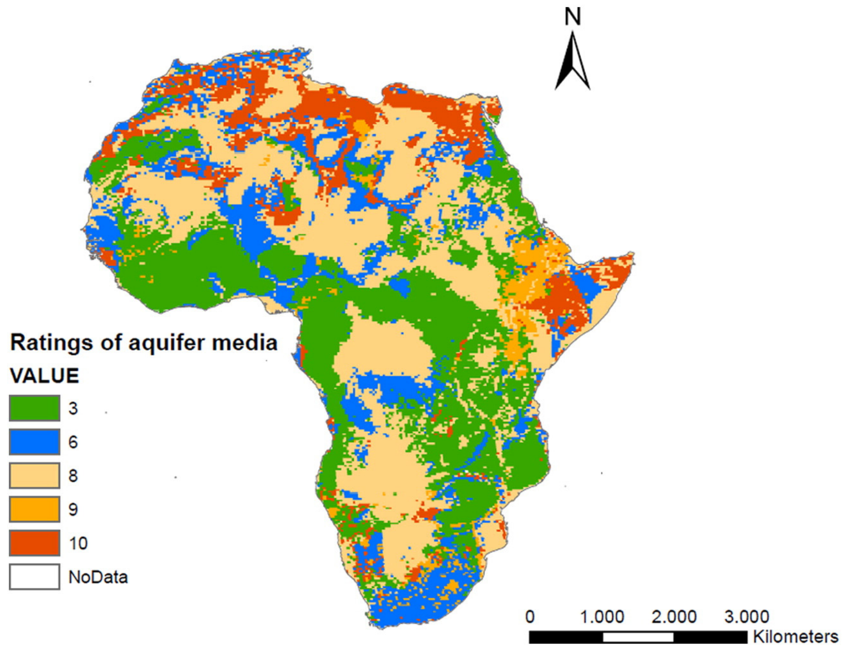

Fig. 6. DRASTIC rating for the Aquifer type (A) for Africa.

DRASTIC vulnerability map. The weight ($L_w = 5$) used for the land use layer is the value defined by Secunda et al. (1998). The land cover/ land use map (Fig. 2) was geo-referenced and also converted to a raster grid format. The twenty two classes of land cover/land use were reclassified into six major classes: forest/tree, croplands, grassland/ shrubland, bare areas, and urban area and water bodies (Fig. 3). Subsequently, land cover/land use was rated according to the values in Table 3.

3.6. Validation using observed nitrate concentration data

The above mentioned modified DRASTIC model is an indirect method for evaluating vulnerability and pollution potential of groundwater systems on a regional scale. This method heavily relies on accessible generic data and should therefore be validated. Indeed, the use of methods that are not validated can result in erroneous conclusions and subjective vulnerability assessment (Leal and Castillo, 2003).

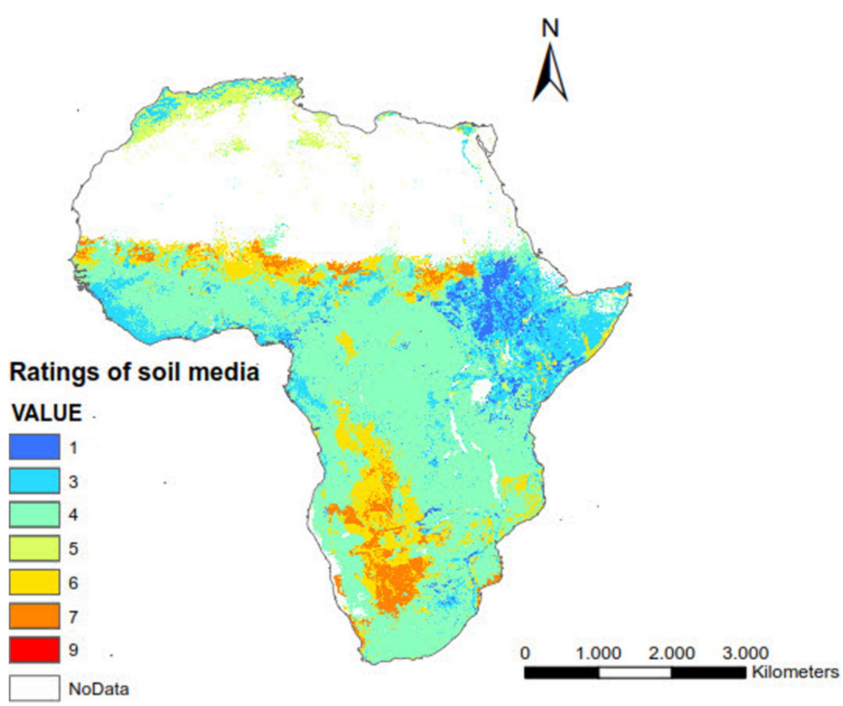

Fig. 7. DRASTIC rating for Soil media (S) for Africa.

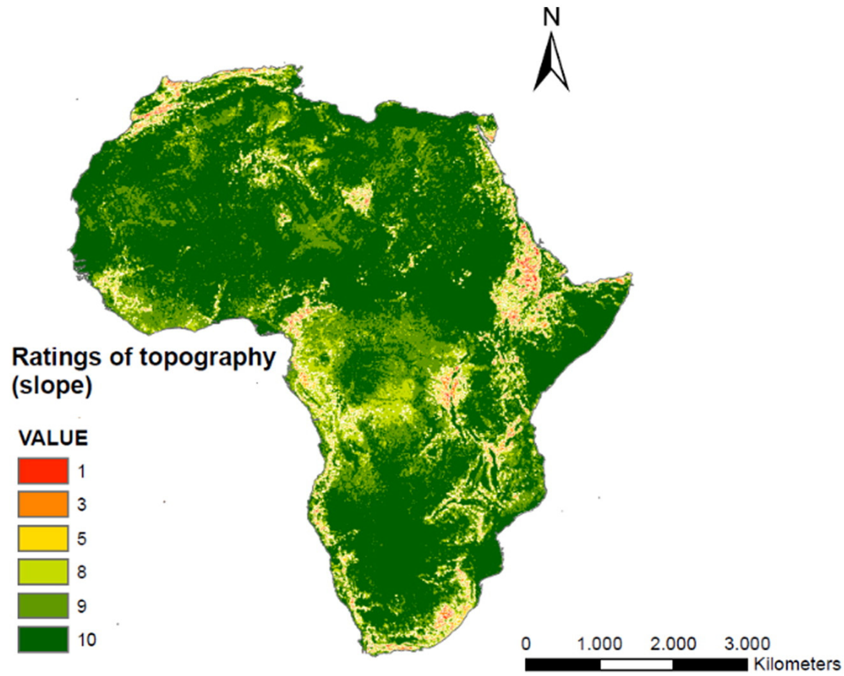

Fig. 8. DRASTIC rating for the Topography (T) for Africa.

However, since intrinsic and specific vulnerabilities only measure the likelihood that groundwater systems may be degraded, or become degraded in the future, it cannot be measured directly in-situ. This challenges the empirical validation of vulnerability mapping (Andreo et al., 2006). In this study we implement the approach as presented by Sulmon et al. (2006), and compare the vulnerability patterns with proxies of vulnerability that can be measured in-situ. In this paper, we use the degradation of groundwater systems by nitrates as a proxy for vulnerability. We select nitrate in groundwater as a proxy since anthropogenic activities like agriculture or urban development are the principle causes of groundwater pollution by nitrates. Also, many groundwater monitoring programs include nitrate as a monitoring parameter, and therefore nitrate contamination data are widely available at the regional scale. The spatial patterns of nitrate contamination are therefore closely related to the spatial patterns of anthropogenic activities and are therefore good proxies for the spatial patterns of overall vulnerability. In our study, we compared groundwater nitrate concentration inferred from a meta-analysis with the aforementioned

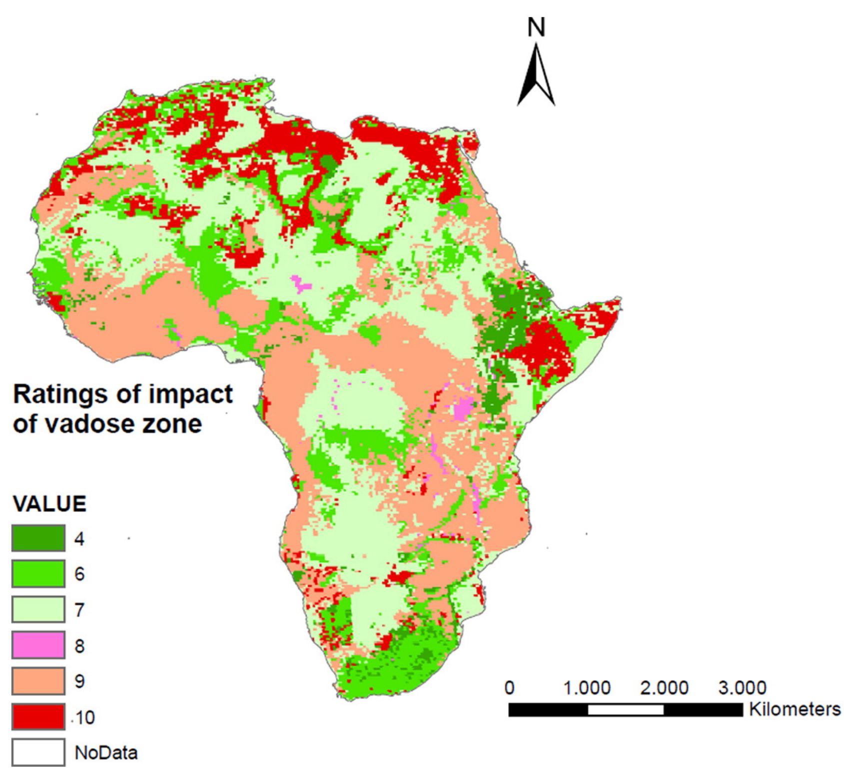

Fig. 9. DRASTIC rating for the Impact of vadose zone (I) for Africa.

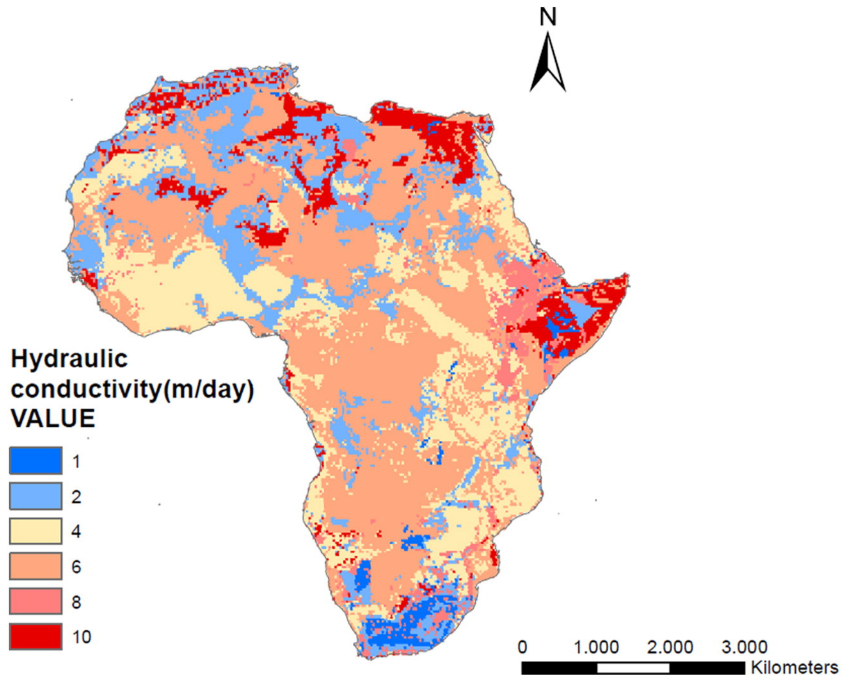

Fig. 10. DRASTIC rating for the hydraulic conductivity (C) for Africa.

modified DRASTIC vulnerability risk map. Existing groundwater nitrate contamination data were collected from 250 studies. This allowed identifying the minimum (185 cases), maximum (206 cases) and mean (92 cases) of nitrate concentration of groundwater systems in Africa. Most studies are situated in the agricultural belt surrounding the African mega-cities where population density is high, or close to the coastal zones.

The validation of the groundwater vulnerability map was made through the nitrate distribution analysis and the vulnerability classes. ArcGIS10.2 was used to distribute spatially the minimum, mean and maximum nitrate concentrations in Africa and were compared with the various degrees of vulnerability maps.

4. Results and discussion

4.1. Ratings of DRASTIC parameters and aquifer vulnerability

Ratings and weights of each parameter of DRASTIC are illustrated in Tables 4 and 5, which vary from 1 to 10, with higher values describing greater pollution.

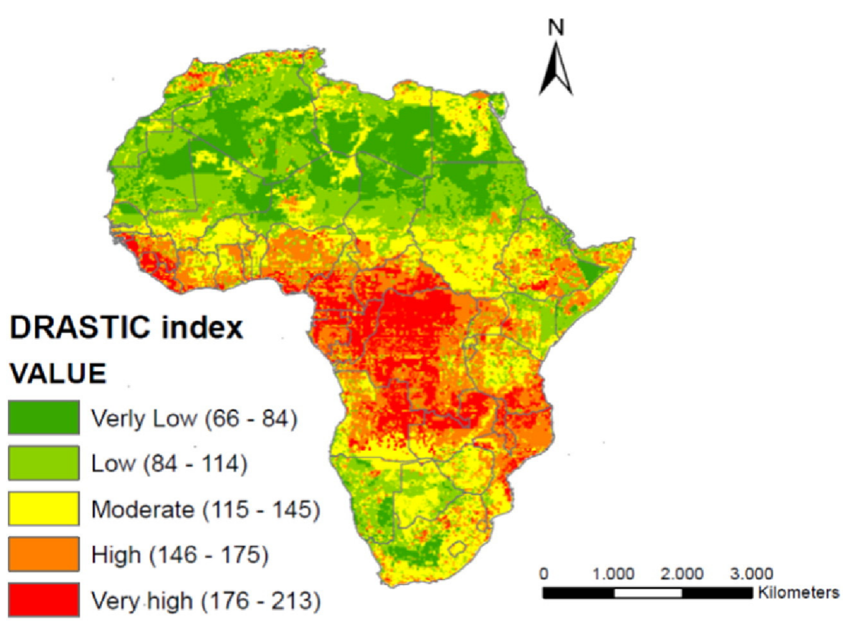

Fig. 11. Groundwater intrinsic vulnerability map of Africa.

The *D* map is represented in Fig. 4. The rate varies from 0 to more than 250 m bgl across the African continent. The heights are shallow mostly in Central Africa, West Africa, Southern Africa and some areas of North Africa. These areas are more susceptible to contamination according the DRASTIC assumptions. The high values of *D* are located in large sedimentary aquifers in North Africa (Libya, Algeria, Egypt and Soudan). These aquifers contain a considerable proportion of Africa's groundwater. The assigned *D* ratings vary between 1 and 10, according the classification of Aller et al. (1987). The highest scores of 9 and 10 are assigned where the depths are in the class 0–7 m and 7–25 m, respectively. The lowest depths are assigned a rating of 1.

The *R* map is shown in Fig. 5. Africa has areas with low net recharge rate (<50 mm/year) for which a rating of 1 is assigned, and areas with high recharge ranges (>225 mm/year), particularly in Central Africa and a portion of western Africa for which a rating of 9 is assigned.

The *A* map is shown in Fig. 6. The ratings in Table 4 are assigned as commonly found in previous studies. A rating of 10 is assigned to carbonate rocks because their permeability value is most likely influenced by the presence of karst phenomena (Gleeson et al., 2011; de Graaf et al., 2014). According Gleeson et al. (2011), volcanic rocks correspond to permeable basalt. A rating of 9 is assigned to these aquifer types. The major aquifer media in unconsolidated sediments are clay, sand and gravel. A rating of 8 is assigned to these media, considering that sand and gravel layers are dominant over clay layers, following the study of MacDonald et al. (2008). A low rating of 3 is assigned to crystalline rocks, because they are identified as fracture igneous/metamorphic rocks. Following Hartmann and Moosdorf (2012), we considered water bodies as an “other rock type”, and we have assigned a rating of 8 for water bodies.

The texture based *S* map is represented in Fig. 7. Soils are mapped in seven different classes. The dominant textures at the continental scale are sandy clay, loam and clay loam. The silty clay and sandy soil types appear in a lower proportion. The highest rating, 9, is assigned to the sandy soil and the lowest rating, 1, to the clayey soil. There is no information available on soils for the Sahara region; thus this part was rated equal to 0.

The *T* map representing the surface slope is shown in Fig. 8. A gentle slope (0–4%) is dominating the largest part of Africa. A rating score of 9 and 10 is assigned to this class, indicating that there is a large probability of pollution infiltration. The highest slopes are located in East Africa and areas associated with the high mountain range. A rate of 1 is assigned to areas where slopes are larger than 18%, indicating their minimal potential effect on the groundwater vulnerability.

The *I* map is shown in Fig. 9. The data used to define this parameter is the same as that used for the *A* map. Although the same hydrolithology is used for both A and I parameters, the maps are different because the crystalline rocks (igneous/metamorphic rocks) of the vadose zone are assigned a rating of 4 for *I* (Aller et al., 1987). The weights and ratings for *I* are shown in Table 4.

The *C* map is shown in Fig. 10. The hydraulic conductivity calculated is inferred from the global permeability database and has been classified in six classes (Fig. 10). In general, the variability of the *C* parameter is not high. Low hydraulic conductivity values, inferior to 0.01 m/day are dominating in Southern Africa. We assigned a rating of 1 to this class. The continent is dominated by the hydraulic conductivities values varying between 0.04–0.13 m/day and 0.13–0.34 m/day, so we assigned respectively the ratings of 4 and 6. The horn of Africa and North Africa shows high conductivity values ranging between 0.57–2.82 m/day. The maximum rating score of 10 is assigned to these areas.

The resultant DRASTIC map is shown in Fig. 11. DRASTIC classes have been grouped together into very low, low, moderate, high and very high vulnerability intervals.

Table 6
Statistical summary of the DRASTIC parameters map.

	D	R	A	S	T	I	C
Minimum	1	1	3	0	1	4	1
Maximum	10	9	13	9	10	13	10
Mean	5.34	2.73	6.36	2.85	9.12	7.68	5.16
SD	3.48	2.52	2.52	2.18	1.69	1.54	2.20
CV(%)	65.16	92.30	39.62	76.49	18.53	20.05	42.67

SD: refers to the standard deviation and CV: coefficient of variation.

Table 7
Statistics of map removal analysis.

Parameters removed	Variation index (%)			
	Minimum	Maximum	Mean	SD
D	0	5	1.28	1.57
R	0	12	1.21	1.23
A	0	4	0.63	0.63
S	0	3	1.15	0.78
T	0	3	0.63	0.53
I	0	8	2.32	1.25
C	0	3	0.40	0.55

One parameter is removed at a time. SD refers to the standard deviation.

4.2. Sensitivity of the DRASTIC model

4.2.1. Summary of the DRASTIC parameters

The Table 6 shows a statistical summary of the seven rated parameters of the DRASTIC model. On average, the *T* parameter (mean = 9.12) has the highest rate values. The *I* (mean = 7.68), *A* (mean = 6.36), *D* (mean = 5.34) *and* C (mean = 5.16) parameter have a moderate rate value. The *S* (mean = 2.85) and *R* (mean = 2.73) parameter imply a low rate value. The coefficients of variation (CV) indicate that a high contribution to the variation of vulnerability is expected by the variability in *R* (92.30%), *S* (76.49%) and *D* (65.16%). A moderate contribution is expected due to variability of *C* (42.67%) and *A* (39.62%), while the impact of the variability of *I* (20.05%) and *T* (18.53%) is expected to be the lowest. In this research, vadose zone and aquifer media are composed of the same material. This could explained why A and I have the same maximum values (Max = 13).

4.2.2. Map removal sensitivity analysis

The results of the map removal sensitivity analysis computed by removing one or more data layers at a time are presented in Tables 7 and 8. Table 7 reveals that the I map is the layer that affects strongly the final vulnerability index. This is mainly due to the high theoretical weight assigned to this parameter (weight = 5). In contrast, Table 6 reveals that the *T* map, A map and C map affects the least the variation index (mean variation = 0.63%, 0.63% and 0.40%, respectively). This is due to the low weight (weight = 1) associated to T and C. The variation in vulnerability observed after the removal of the *D*, and *R* map is moderate (mean = 1.28%, and 1.21% respectively).

Table 8 illustrates the variation of the vulnerability index due to the removal of one or more data layers at a time from the DRASTIC model computation. The layer which causes less variation in the final vulnerability index is removed first. It appears from Table 7 that after removing the topography layer, T, the variation index has the least average value (mean = 0.63%), while the highest variation is associated with the

Table 8
Statistics of map removal sensitivity.

Parameters used	Variation index (%)			
	Mean	Minimum	Maximum	SD
D, R, A, S, I, C	0.63	0	3	0.53
D, R, S, I, C	1.14	0	4	1.11
D, R, I, C	3.2	0	8	1.98
D, I, C	6.84	0	30	3.13
D, I	11.31	0	46	5.34
I	17.21	0	47	7.50

One or more parameters are removed at a time. SD refers to the standard deviation.

Table 9
Statistics of single parameter sensitivity analysis.

Parameters	Theoretical weight	Theoretical weight (%)	Effective weight (%)			
			Mean	Min	Max	SD
D	5	21.7	19.71	2	70	11.52
R	4	17.4	7.25	2	32	5.94
A	3	13.0	15.76	4	39	7.43
S	2	8.7	3.92	0	17	3.32
T	1	4.3	7.19	0	13	2.31
I	5	21.7	31.12	11	60	7.49
C	3	13.0	12.07	1	33	5.44

SD refers to the standard deviation.

removal of the D and I parameters (mean = 11.31% and mean = 17.21% respectively). This average variation index changes as more data layers are removed from the computation. The removal of some layers (D, and I) affects the vulnerability assessment and this is demonstrated by all sensitivity tests.

4.2.3. Single-parameter sensitivity analysis

While the map removal sensitivity analysis presented in previous section has confirmed the significance of the seven parameters in the assessment of the DRASTIC vulnerability index at the pan Africa scale, the single parameter sensitivity analysis allows the comparison between the effective and theoretical weights. The effective weight of the DRASTIC parameter is a function of the theoretical weight and the interaction with the other six parameters of the DRASTIC model (Babiker et al., 2005). The comparison is given in Table 9. The effective weight of the DRASTIC parameters obtained in this study exhibited some deviation from the theoretical weights. The *I* parameter tends to be the most effective parameter in the vulnerability assessment. His mean effective value of 31.12% is higher than the theoretical weight of 21.7%. This result is in agreement with the map removal sensitivity analysis for this parameter. The effective weight of the D parameter (19.71%) is less than to its theoretical weight 21.7%. The effective weights for *A* and *T* (15.76%, 7.19%) are higher than their theoretical weight (13.0%, 4.3%). The significance of the vadose zone, aquifer media and topography layers highlights the importance of obtaining accurate, detailed and representative information about these factors. The other DRASTIC parameters reveal lower effective weights compared to their theoretical weights. Parameters A, I and C are based effectively on the same datasets, which explains their contribution to adding up more 50% of the effective weight of the intrinsic vulnerability.

4.3. Mapping of groundwater pollution risk

The result of groundwater pollution risk map is shown in Fig. 12. We classified Africa into five zones corresponding to a very low, low, moderate, high and very high groundwater pollution risk. We observe a very low and low risk for the Sahara desert where large sedimentary basins are found. Indeed, the absence of important anthropogenic activities in combination with very low and low vulnerability zones result in very low and low contamination risks. We calculate high to very high vulnerability zones for regions in North Africa and a few zones of Eastern Africa and Southern Africa. A large part of Southern Africa shows a low risk for pollution. In general, high risk areas for pollution in Africa are lowlands where agricultural development is important. A region with a low pollution risk does not mean that it is free from groundwater contamination, but that it is relatively less susceptible to contamination compared to other regions.

The intrinsic vulnerability map indicated that Central Africa and a portion of West Africa are dominated by very high and high intrinsic vulnerabilities. The low depth of groundwater in these regions and the high recharge explains this high intrinsic vulnerability. The large sedimentary basins in North Africa are characterized by a low intrinsic vulnerability. The large depths of water and very low recharge rates explain these low intrinsic vulnerabilities. It also appears that in some regions like Southern Africa and Eastern Africa, a very high and high vulnerability of groundwater are also due to the shallow depths of groundwater systems. The topography parameter had the highest mean rating value for assessing the intrinsic vulnerability of Africa groundwater. The impact of vadose zone, the aquifer media and depth to groundwater had a moderate mean rating value while the soil media, the net recharge and the hydraulic conductivity had a low mean rating value respectively on vulnerability. The map removal sensitivity analysis test indicated that the vulnerability index is highly sensitive to the removal of the impact of vadose zone, the depth to groundwater and hydraulic conductivity layers. The index is less sensitive to the removal of topography parameter. The single-parameter sensitivity analysis showed that the

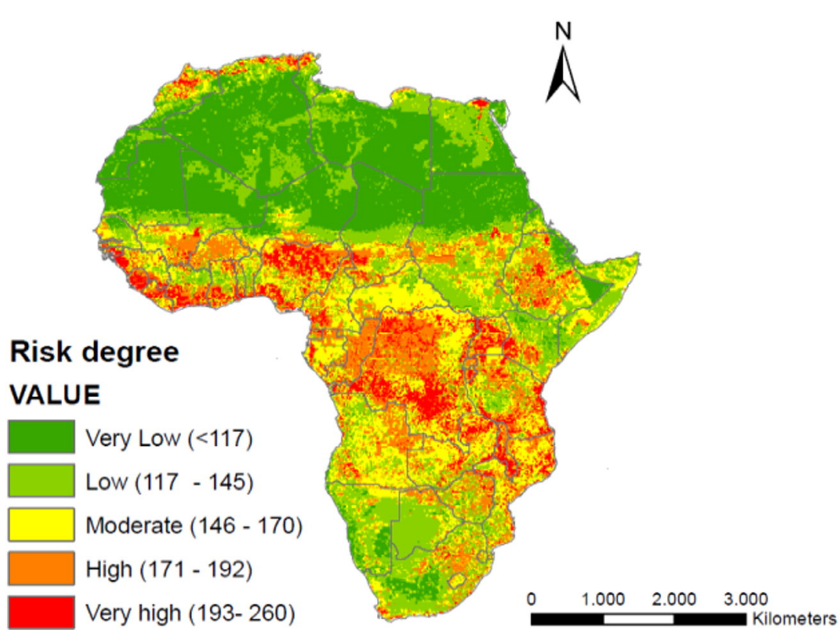

Fig. 12. Risk map of groundwater pollution for Africa.

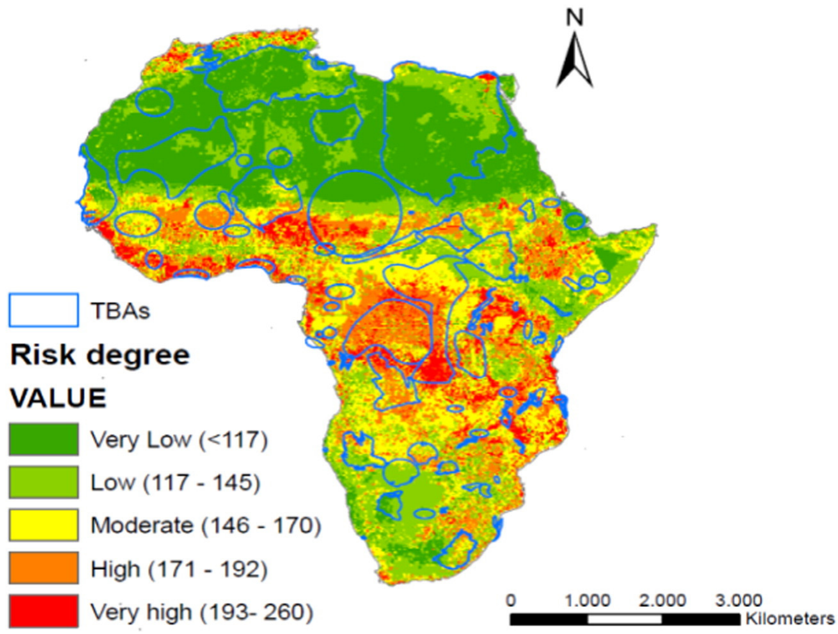

Fig. 13. Risk map overlaying Transboundary aquifers (TBAs) defined by Altchenko and Villholth (2013).

impact of vadose zone, the aquifer media and topography are the most significant environmental parameters which dictate the intrinsic vulnerability of African aquifers. Consequently, this highlights the importance of obtaining accurate, detailed, and representative information for the different parameters explaining intrinsic vulnerability of groundwater systems (Bouchaou et al., 2009).

We also created the first pan African groundwater pollution risk map. Areas under very high and high pollution risk are mainly characterized by shallow groundwater systems. At the opposite, low contamination risks are observed for the large sedimentary basins in North Africa, a little portion of Eastern and Southern Africa. Indeed, these groundwater systems situates at larger depths. The risk map of groundwater pollution in Africa shows that water resources are mainly under pressure in large agricultural basins.

The eight model parameters of the groundwater pollution risk model were constructed, classified and encoded employing various maps from several sources and at different mapping scales. Fig. 12 has the merit to produce a very valuable map for managing and protecting groundwater at the regional scale. So, water directors can use the vulnerability map to support the design of groundwater development or protection programs. Fig. 13 for example give the utility of this risk map for transboundary aquifers management (International Network of Basin Organizations (INBO), Global Water Partnership (GWP)).

4.4. Validation of the groundwater vulnerability map

4.4.1. Spatial concentrations of nitrate

The spatial distribution of the nitrate mean groundwater concentration inferred from the meta-analysis is illustrated in Fig. 14. In the meta-analysis database, 206 studies related to the maximum concentration of nitrate, 185 studies to the minimum concentration of nitrate, and 92 studies to the mean concentration of nitrate have been analyzed. This meta-analysis reveals that nitrate concentration varies between zero

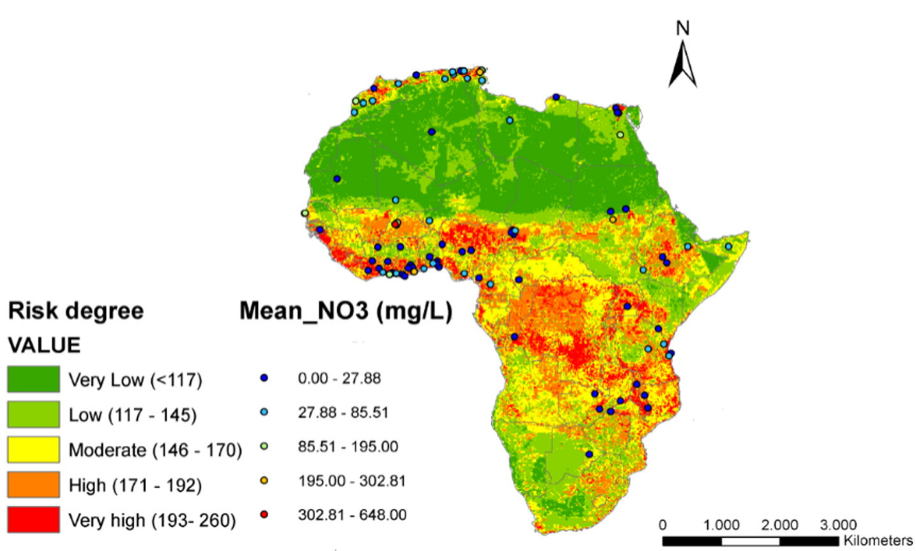

Fig. 14. Spatial distribution of mean nitrate concentration in groundwater.

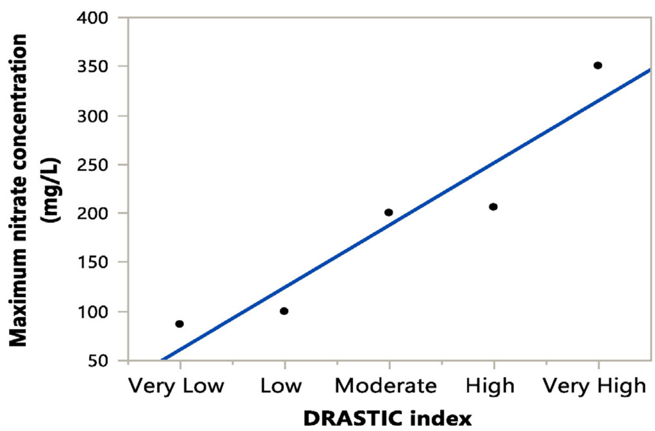

Fig. 15. Relation between nitrate maximum and DRASTIC with $R^2 = 0.89$.

and 4625 mg/L. We selected the mean nitrate concentration as proxy for risk and superimposed on the previously developed risk map.

4.4.2. Regression of aggregated nitrate concentration data with estimated groundwater risk

We also aggregated the observed maximum nitrate concentration for each vulnerability class and compared it with vulnerability and risk. In this approach, the DRASTIC index has been used as surrogate of the vulnerability map and regressed against the extracted nitrate concentration. Figs. 15 and 16 illustrate that the aggregated maximum nitrate concentration data are positively related to the intrinsic vulnerability ($R^2 = 0.89$) and the risk for pollution ($R^2 = 0.65$) respectively. This suggests that the generic model for mapping vulnerability and groundwater pollution risk is consistent with observed nitrate inferred from the literature. We chose the maximum concentration values of nitrate as aggregate values to show the trend of our groundwater vulnerability model, because the sample size is larger for the maximum concentration. Also, sample data of maximum concentration cover the complete study area. However, the aforementioned results shows that further validation using more measurement data is recommended.

5. Conclusions

We assessed the intrinsic vulnerability and risk for groundwater pollution at the pan African scale. We deployed the empirical index model DRASTIC into a GIS. The GIS provides an effective analysis environment and a strong capacity for handling large amounts of spatial data. We identified the seven environmental DRASTIC parameters (Depth to water (D), net Recharge (R), Aquifer media (A), Soil media (S), Topography (T), Impact of vadose zone (I), and hydraulic Conductivity (C)) from available generic data, and compiled them into a 15 km resolution geo-

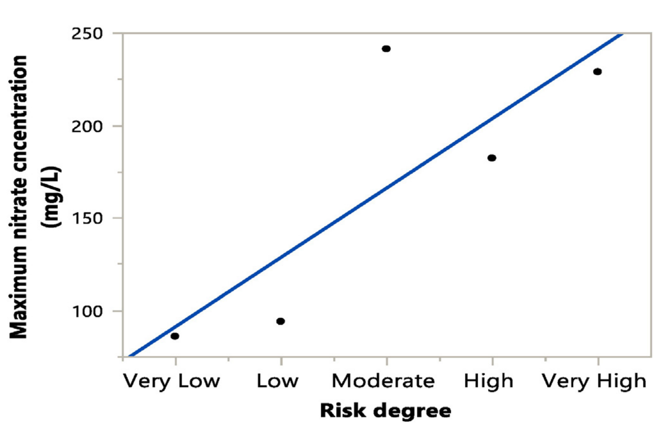

Fig. 16. Relation between nitrate maximum and risk degree with $R^2 = 0.65$.

database for the African continent. We classified and coded these parameters to create an intrinsic groundwater vulnerability map. Subsequently, we combined the intrinsic vulnerability map with a high resolution land use/land cover map to assess the groundwater pollution risk. We show that the DRASTIC index varies between 66 and 213. We classified this index into 5 classes, ranging from very low to very high.

Despite the lack or limit of groundwater pollution data at the continental scale, the intrinsic vulnerability and risk map was tested and validated using nitrate concentration data as proxies for vulnerability and risk. Nitrate concentration data were inferred from a literature meta-analysis. High nitrate concentrations detected in literature coincide with high intrinsic vulnerability and high pollution risks. This illustrates the consistency between the calculated vulnerability and groundwater pollution risk using generic data on the one hand, and the observed contamination on the other hand. However, the explained variability in the boxplots and scatter plots is still rather low, showing that quite some scope exist to calibrate and to improve the proposed vulnerability and groundwater risk mapping procedure. This should be based on a better understanding of the factors explaining the contamination at the pan African scale, and the availability of monitoring data allowing to consolidate the calibration and validation of the presented mapping methodologies.

The maps that were designed in this study can increase awareness of citizens and regulators in areas where groundwater pollution is likely to be significant. In addition, they could prompt national or international authorities to foster targeted local investigations. In fact, environmental management needs to be operatively performed at regional and local scales, but investment policies can be addressed at continental or even global scales by international agencies and authorities (e.g., FAO, UNEP, and OECD). The map should serve as a general guideline for planners and decision-makers with land-use and water management development issues.

Acknowledgments

This research was carried out within the framework of a Ph.D. The authors are thankful to Islamic Development Bank (IDB) group for granting a PhD research Merit Scholarship Program (MSP) to the first author. Several people from over the world helped with data acquisition, which were P. Döll Petra and F. Portman (Frankfurt University), T. Gleeson (McGill University) and N. Moosdorf (Hamburg Germany). We thank very much H. Sellami.

References

Al-Hanbali, A., Kondoh, A., 2008. Groundwater vulnerability assessment and evaluation of human activity impact (HAI) within the Dead Sea groundwater basin, Jordan. Hydrogeology Journal 16 (3), 499–510.

Aller L, Bennet, T., Leher, J.H, Petty, R.J & Hackett G. (1987). DRASTIC: A Standardized System for Evaluating Ground Water Pollution Potential Using Hydrogeological Settings. U.S. Environmental Proctection Agency, Ada Oklahoma 74820, EPA 600/2-87-035, 662 pp.

Aller, L., Bennet, T., Lehr, J. H., and Petty, R. J., (1985). DRASTIC: A Standardized System for Evaluating Groundwater Pollution Using Hydrological Settings. Ada, OK, USA: Prepared by the National Water Well Association for the US EPA Office of Research and Development. EPA/600/2-85-018, 163pp.

Altchenko, Y., Villholth, K.G., 2014. Mapping irrigation potential from renewable groundwater in Africa – a quantitative hydrological approach. Hydrology and Earth System Sciences Discussions 11 (6), 6065–6097.

Altchenko, Y.V., Villholth, K.G., 2013. Transboundary aquifer mapping and management in Africa: a harmonised approach. Hydrogeology Journal 21 (7), 1497–1517.

Alwathaf, Y., 2011. Assessment of Aquifer Vulnerability Based on GIS and ARCGIS Methods: A Case Study of the Sana'a Basin (Yemen). Journal of Water Resource and Protection 03 (12), 845–855.

Andreo, B., et al., 2006. Karst groundwater protection: First application of a Pan-European Approach to vulnerability, hazard and risk mapping in the Sierra de Libar (Southern Spain). Sci. Total Environ. 357 (1–3), 54–73.

Ateawung, Juilius Nkezeah. (2010). A GIS based water balance study of Africa. Master Science. University Gent. Belgium, 55pp.

Babiker, I.S., et al., 2005. A GIS-based DRASTIC model for assessing aquifer vulnerability in Kakamigahara Heights, Gifu Prefecture, central Japan. Sci. Total Environ. 345 (1–3), 127–140.

Bonsor, H. C. and MacDonald, A. M. (2011). An initial estimate of depth to groundwater across Africa. British Geological Survey Open Report, OR/11/067, 26pp.
Bouchaou, et al., 2009. Origin and residence time of groundwater in the Tadla basin (Morocco) using multiple isotopic and geochemical tools. J. Hydrol. 379 (3–4), 323–338.
Chilton, P. J. and SD. Foster, S. (1995). Hydrogeological characterisation and water-supply potential of basement aquifers in tropical Africa. Hydrogeology Journal, 3(1), 36–49.
de Graaf, I.E.M., Sutanudjaja, E.H., van Beek, L.P.H., Bierkens, M.F.P., 2014. A high resolution global scale groundwater model. Hydrology and Earth System Sciences Discussions 11 (5), 5217–5250.
Defourny, P., Kirches, G., Brockmann, C., Boettcher, M., Peters, M., Bontemps, S., et al., 2014. Land cover CCI product user guide version 2.
Dickerson, J. Ryan (2007). A Modified Drastic Model for Siting Confined Animal Feeding Operations (CAFOS) in Williams County, Ohio. A Thesis Master of Science, College of Bowling Green State University, 46pp.
Döll, P., Fiedler, K., 2008. Global-scale modeling of groundwater recharge. Hydrol. Earth Syst. Sci. 12, 863–885.
Dürr, H.H., Meybeck, M., Dürr, S.H., 2005. Lithologic composition of the Earth's continental surfaces derived from a new digital map emphasizing riverine material transfer. Global Biogeochem. Cycles 19. http://dx.doi.org/10.1029/2005GB002515.
Ehteshami, M., Peralta, R.C., Eisele, H., Deer, H., Tindall, T., 1991. Assessing pesticide contamination to groundwater: a rapid approach. Journal of Ground Water 29 (6), 939–944.
Ersoy, A.F., Gültekin, F., 2013. DRASTIC-based methodology for assessing groundwater vulnerability in the Gümüşhacıköy and Merzifon basin (Amasya, Turkey). Earth sciences research journal 17 (1), 33–40.
Evans, B.M., Myers, L.W., 1990. A GIS-based approach to evaluating regional groundwater pollution potential with DRASTIC. J. Soil Water Conserv. 45 (2), 242–245.
Farjad, B., Mohamed, T.A., Wijesekara, N., Pirasteh, S., Shafri, H.Z.B.M., 2012. Groundwater intrinsic vulnerability and risk mapping. Proceedings of the ICE — Water Management 165 (8), 441–450.
Fritch, T.G., McKnight, C.L., Yelderman Jr, J.C., Arnold, J.G., 2000. An aquifer vulnerability assessment of the Paluxy aquifer, central Texas, USA, using GIS and a modified DRASTIC approach. Environ. Manag. 25 (3), 337–345.
Gleeson, T.S., Leslie, Moosdorf, N., Hartmann, J., Dürr, H.H., Manning, A.H., van Beek, L.P.H., Jellinek, A.M., 2011. Mapping permeability over the surface of the earth. Geophys. Res. Lett. 38 (2), L02401. http://dx.doi.org/10.1029/2010GL045565.
Gleeson, T., Moosdorf, N., Hartmann, J., Beek, L., 2014. A glimpse beneath earth's surface: GLobal HYdrogeology MaPS (GLHYMPS) of permeability and porosity. Geophys. Res. Lett. 41 (11), 3891–3898.
Gogu, R.C., Dassargues, A., 2000. Current and future trends in groundwater vulnerability assessment. Environ. Geol. 39 (6), 549–559.
Hartmann, J., Moosdorf, N., 2012. The new global lithological map database GLiM: a representation of rock properties at the Earth surface. Geochem. Geophys. Geosyst. 13 (12), Q12004. http://dx.doi.org/10.29/2012GC004370.
Hasiniaina, F., Zhou, J., Guoyi, Z.L., 2010. Regional assessment of groundwater vulnerability in tamtsag basin, Mongolia using drastic model. Journal of American Science 6 (11), 65–78.
Hengl, T., et al., 2014. SoilGrids1km — global soil information based on automated mapping. PLoS One 9 (8), e105992.
Jourda J. P., Kouame K. J., Adja M.G., Deh S. K., Anani A. T., Effini A. T., Biemi J. (2007). Evaluation du degré de protection des eaux souterraines : vulnérabilité à la pollution de la nappe de Bonoua (Sud-Est de la Côte d'Ivoire) par la méthode DRASTIC, Conférence Francophone ESRI, 10–11 Octobre-Versailles, 8pp.
Leal, J.A.R., Castillo, R.R., 2003. Aquifer vulnerability mapping in the turbio river valley, Mexico: a validation study. Geofísica Internacional 42 (1), 141–156.
Lee, S., 2003. Evaluation of waste disposal site using the DRASTIC system in Southern Korea. Environ. Geol. 44 (6), 654–664.
Liggett, J., Gilchrist, A., 2010. Technical summary of intrinsic vulnerability mapping methods in the regional districts of Nanaimo and Cowichan valley. Geological Survey of Canada, Open File 6168 64p.
Lodwick, W.A., Monson, W., Svoboda, L., 1990. Attribute error and sensitivity analysis of map oprations in geographical information systems: suitability analysis. Int J Geogr Inf Syst; 4 (4), 413–428.
MacDonald A.M. et al. (2011). Groundwater resilience to climate change in Africa. British Geological Survey (BGS) Open Report, Open Report, (OR/11/031), 25 pp 2011.
MacDonald, A.M., et al., 2012. Quantitative maps of groundwater resources in Africa. Environ. Res. Lett. 7 (2), 024009.
MacDonald, A., Davies, J., Callow, R.C., 2008. African hydrogeology and rural water supply. In: Adelana, S., MacDonald, A. (Eds.), Applied Groundwater Studies in Africa. CRC Press, Leiden, The Netherlands, pp. 127–148 (IAH selected papers on hydrogeology, 13).
Mao, Yuan-yuan, Zhang, Xue-gang, Wang, Lian-sheng, 2006. Fuzzy pattern recognition method for assessing groundwater vulnerability to pollution in the Zhangji area. J. Zhejiang Univ. Sci. B. 7 (11), 1917–1922.
Mayaux, P., Bartholomé, E., Massart, M., Van Cutsem, C., Cabral, A., Nonguierma, A., et al. (2003). A land cover map of Africa. European Commission, Joint Research Centre, EUR20665EN, 56pp.
Merchant, J.W., 1994. GIS-based groundwater pollution hazard assessment: a critical review of the DRASTIC model. Photogramm. Eng. Remote. Sens. 60 (9), 1117–1127.
Mimi, Z.A., Mahmoud, N., Madi, M.A., 2011. Modified DRASTIC assessment for intrinsic vulnerability mapping of karst aquifers: a case study. Environmental Earth Sciences 66 (2), 447–456.
Musekiwa, C., Majola, K., 2013. Groundwater vulnerability map for South Africa. South African Journal of Geomatics 2 (2), 152–163.
Napolitano, P. and & Fabbri, A. G. (1996). Single-parameter sensitivity analysis for aquifer vulnerability assessment using DRASTIC and SINTACS. Application of Geographic Information Systems in Hydrology and Water Resources Management (Proceedings of the Vienna Conference, April 1996). IAHS Publ. no.235 Appril 1996, 559–566.
Neshat, A., Pradhan, B., Pirasteh, S., Shafri, H.Z.M., 2014. Estimating groundwater vulnerability to pollution using a modified DRASTIC model in the Kerman agricultural area. Iran. Environ. Earth Sci. 71 (7), 3119–3131.
National Research Council, 1993. Groundwater Vulnerability Assessment, Contaminant Potential Under Conditions of Uncertainty. National Academy Press, Washington DC.
Pavelic, P., Giordano, M., Keraita, B., Ramesh, V; Rao, T. (Eds.). (2012). Groundwater availabilityand use in Sub-Saharan Africa: a review of 15 countries. Colombo, Sri Lanka: InternationaWater Management Institute (IWMI). doi:http://dx.doi.org/10.5337/2012.213 (274 p.).
Rahman, A., 2008. A GIS based DRASTIC model for assessing groundwater vulnerability in shallow aquifer in Aligarh, India. Appl. Geogr. 28, 32–53.
Rosen, L., 1994. A study of the DRASTIC methodology with emphasis on Swedish conditions. Groundwater 32 (2), 278–285.
Saidi, S., Bouri, S., Ben Dhia, H., 2010. Groundwater vulnerability and risk mapping of the Hajeb-jelma aquifer (Central Tunisia) using a GIS-based DRASTIC model. Environmental Earth Sciences 59 (7), 1579–1588.
Saidi, S., Bouri, S., Ben Dhia, H., 2011. Sensitivity analysis in groundwater vulnerability assessment based on GIS in the Mahdia-Ksour Essaf aquifer, Tunisia: a validation study. Hydrol. Sci. J. 56 (2), 288–304.
Secunda, S., Collin, M., Melloul, A.J., 1998. Groundwater vulnerability assessment using a composite model combining DRASTIC with extensive land use in Israel's Sharon region. J. Environ. Manage. 54, 39–57.
Seguin, J.J., 2008. Carte Hydrogeologique de l'Afrique à l'échelle du 1/10M. Orléans: Bureau de Recherches Géologiques et Minières (BRGM).
Sener, E., Sener, S., Davraz, A., 2009. Assessment of aquifer vulnerability based on GIS and DRASTIC methods: a case study of the Senirkent-Uluborlu Basin (Isparta, Turkey). Hydrogeol. J. 17, 2023–2035.
Senthilkumar, P., Nithya, J., Babu, S.S., 2014. Assessment of Groundwater Vulnerability in Krishnagiri District, Tamil Nadu, India Using DRASTIC Approach. International Journal of Innovative Research in Science, Engineering and Technology 3 (3).
Shirazi, S.M., Imran, H.M., Akib, S., 2012. GIS-based DRASTIC method for groundwater vulnerability assessment : a review. Journal of Risk Research 15 (8), 991–1011.
Shukla, S., Mostaghimi, S., Shanholt, V.O., Collins, M.C., Ross, B.B., 2000. A county-level assessment of ground water contamination by pesticides. Groundwater Monitoring & Remediation 20 (1), 104–119.
Struckmeier W and Richts A (2008). Groundwater resources of the world 1: 25 000 000 (Hannover: World-wide Hydrogeological Mapping and Assessment Programme (WHYMAP))
Sulmon, R., Leterme, B., Pinte, D., Vanclooster, M., Bogaert, P., 2006. Can groundwater vulnerability maps be validated? In: Laftouhi, N. (Ed.), Gestion intégrée des ressources en eau et défi au développement durable (GIRE3D). Marrakech, Morocco May 2006.
UNEP. (2010). "Africa water atlas". Division of Early Warning and Assessment (DEWA). United Nations Environment Programme (UNEP). Nairobi, Kenya.
Uricchio, V.F., Giordano, R., Lopez, N., 2004. A fuzzy knowledge-based decision support system for groundwater pollution risk evaluation. J. Environ. Manage. 73, 189–197.
Vanclooster, M., Mfumu, K.A., Ouedraogo, I., 2014. L'union fait la force or how different approaches should be combined to assess groundwater vulnerability at the regional scale. IAH (Marrakech, Maroc, du 15/09/2014 au 19/09/2014).
Villholth, K.G., Tottrup, C., Stendel, M., Maherry, A., 2013. Integrated mapping of groundwater drought risk in the Southern African Development Community (SADC) region. Hydrogeol. J. http://dx.doi.org/10.1007/s10040-013-0968-1.
Voudouris, K., 2009. Assessing groundwater pollution risk in sarigkiol basin, NW Greece. In: Gallo, M., Herrari, M. (Eds.), River Pollution Research Progress. Nova Science Publishers Inc., pp. 265–281 Chapter 7.
Vrba, J., Zaporozec, A., 1994. Guidebook on Mapping Groundwater Vulnerability. 16. International Association of Hydrogeologists, Hannover, Germany 131pp.
Wright, E.P., 1992. The hydrogeology of crystalline basement aquifers in Africa. Geol. Soc. Lond., Spec. Publ. 66 (1), 1–27.
Xu Yongxin and Brent Usher. (2006). Groundwater Pollution in Africa. Taylor and Francis/ Balkema, ISBN 10:415-41167-X.UK The Netherlands, 353pp.